



Thermal analysis of W-free Co–(Ni)–Al–Mo–Nb superalloys

Damian Migas¹ · Grzegorz Moskal¹ · Tomasz Maciąg²

Received: 16 August 2019 / Accepted: 21 January 2020 / Published online: 24 February 2020
© The Author(s) 2020

Abstract

In this investigation, the thermal analysis of W-free cobalt-based superalloys based on Co–Al–Mo–Nb and Co–Ni–Al–Mo–Nb systems was performed. The analysis was performed at different stages of heat treatment process. The differential thermal analysis (DTA) was utilized for the determination of characteristic temperatures related to microstructural changes. First of all, the DTA analysis was carried out for discussing as-cast alloys in the temperature range of 40–1500 °C. The results showed thermal effects connected with melting and important order–disorder transition. The temperature range of 1200–1250 °C was chosen for performance of a first heat treatment operation for the investigated alloys. Specimens were annealed at selected temperature for 5 h. The microstructure of alloys after solution heat treatment was analyzed as well. Afterward, the solutionized specimens were subjected to the further thermal analysis in order to select the aging temperature according to the order–disorder transformation related to formation of γ' phase with overall formula $\text{Co}_3(\text{Al},\text{X})$. Five aging variants were performed in the temperature range of 800–1000 with a step of 50 °C. After each stage of heat treatment, SEM/EDS analysis and hardness measurements were performed.

Keywords γ/γ' · Precipitation hardening · W-free superalloys · Cobalt · DTA

Introduction

The starting point of development of the new creep-resistant materials based on Co was discovery of the two-phase area in the ternary system Co–Al–W. This field consists of γ matrix based on Co with fcc type of lattice and L1_2 intermetallic phase with overall formula $\text{Co}_3(\text{Al},\text{W})$. This fact gets the possibility of creation of a new group of Co-based superalloys strengthened by L1_2 intermetallic phase with microstructure very similar to conventional Ni-based superalloys of γ/γ' type [1, 2]. There are two basic groups of these alloys at this time. First of them is based on tungsten addition and $\text{Co}_3(\text{Al},\text{W})$ phase as a strengthening structural element. The second group is called W-free alloys and consists

of other high melting point elements such as Mo, Nb and Ta as elements forming the desirable $\text{Co}_3(\text{Al},\text{X})$ phase [3, 4].

There are many articles related to those alloys, focused on microstructure, mechanical properties, oxidation, creep resistance and the influence of quaternary and quinary alloying elements on those properties. However, in the literature data exists relatively low information about heat treatment parameters and such processes as homogenization solutionizing and aging [5–12]. Only in few publications, it is possible to find the information about the influence of alloying elements on *solidus* temperature of Co–Al–W alloys, and especially *solvus* temperature of strengthened structural elements of L1_2 type. This information is related mainly to W and Al concentration and eventually to Ni addition as an alloying element.

This article concerns the influence of W-replacement by Mo and Nb on the thermal effects in Co-based superalloys. Some data regarding W-free superalloys are available in the literature [3, 13, 14]. The similar alloys based on Co–Al–Mo–Nb and Co–Ni–Al–Mo–Nb systems were prepared by induction vacuum melting. The thermal analysis of discussed superalloys was performed in as-cast state as well as on further stages of heat treatment. Moreover, after each heat treatment step, the microstructure of alloys was

✉ Damian Migas
damian.migas@polsl.pl

¹ Department of Advanced Materials and Technologies, Faculty of Materials Engineering, Silesian University of Technology, Krasińskiego 8 St., 40-019 Katowice, Poland

² Department of Metallurgy and Recycling, Faculty of Materials Engineering, Silesian University of Technology, Krasińskiego 8 St., 40-019 Katowice, Poland

investigated. The influence of W-replacement on thermal behavior of Co-based alloys including determination of *solidus* and *solvus* temperatures was analyzed.

Materials and methods

The Co–10Al–5Mo–2Nb and Co–20Ni–10Al–5Mo–2Nb (at%) alloys were melted using induction vacuum furnace VSG 02 Balzers and cast under Ar atmosphere. Pure metals were used in the investigation, including Co (min. 99.98%), Al (99.98%) Mo (99.98%) and Nb (99.99). Mo and Nb were being dosed to liquid bath of Co and Al. The alloys were melted in the temperature range of 1600–1700 °C for the time of approx. 10 min. The investigated alloys were cast into cold graphite molds under the protective gas (Ar). The time of solidification did not exceed 10 s. In the next step, metal pieces were cut from the cast ingot; samples for heat treatment investigations were prepared. The solution heat treatment was performed at 1200 °C for 5 h with subsequent quenching in water. The solution heat treatment operation was carried out in a laboratory furnace with the Ar protection atmosphere. Afterward, the solutionized specimens were subjected to aging at temperatures of 800, 850, 900, 950, 1000 °C for 5 h in the Ar atmosphere with final water quenching.

The thermal analysis including differential thermal analysis (DTA) was carried out on the as-cast, solutionized and aged specimens. The DTA analysis was carried out using the NETZSCH STA 449 F3 Jupiter thermal analyzer. The temperature range of analysis was 40–1500 °C of heating and cooling rate 20 °C min⁻¹. As a reference, an empty alumina crucible was used. Additionally, differential scanning calorimetry (DSC) was used in order to investigate temperature of order–disorder transformation in alloys. The measurements in the temperature range of 40–1200 °C were performed using multi-HTC high-temperature calorimeter from Setaram. The measurements were performed under the Ar protection; the heating rate was 5 °C min⁻¹.

The specimens for microstructure evaluation were prepared by grinding, polishing and chemical etching. In the case of as-cast and as-solutionized samples, a reagent containing 25 mL H₂O, 50 mL HCl, 15 g FeCl₃ i 3 g CuCl₂ × NH₄Cl₂ × H₂O was used for etching. The specimens after aging were chemically etched using reagent containing 80 mL of lactic acid, 10 mL of HNO₃ and 10 mL of H₂O₂. The as-cast microstructure was analyzed by means of optical microscopy (OM), scanning electron microscopy (SEM) and X-ray diffraction (XRD). The optical micrographs were performed using the Nikon Eclipse MA200 microscope. In the case of SEM/EDS analysis, the scanning electron microscope (SEM, Hitachi S-3400 N) equipped with the energy dispersion spectrometer (EDS, Thermo

Noran System Seven) was utilized. The phase composition was evaluated using Phillips X'Pert³ Powder diffractometer. Furthermore, hardness of specimens was investigated by Vickers method. The measurements were performed using the ZWICK ZHV TKV5030 Vickers hardness tester using a load of 2.5 kg. The analogous research methodology was utilized for the specimens after solution heat treatment and aging.

Results and discussion

The first part of work concerns concise description of the as-cast microstructure of investigated alloy. In the case of Co–10Al–5Mo–2Nb (at%) alloy, the characterization of primary microstructure is available [15], whereas the as-cast microstructure of second alloy is similar. The OM and SEM micrographs of investigated alloys in the as-cast state can be observed in Fig. 1. Both alloys are characterized by a dendritic microstructure, typical for the castings made with high cooling rate. For cobalt alloys in which W was replaced by Mo and Nb, occurrence of some eutectic phases in the interdendritic regions may be observable (phases are indicated by white arrows). Taking into account the chemical and phase composition of the alloys after casting (Fig. 2), the interdendritic spaces may be enriched in Co₃X phases (where X = Mo, Nb). Such phases were detected via X-ray diffraction analysis. For the alloy with composition Co–20Ni–10Al–5Mo–2Nb (at%), peaks related to the

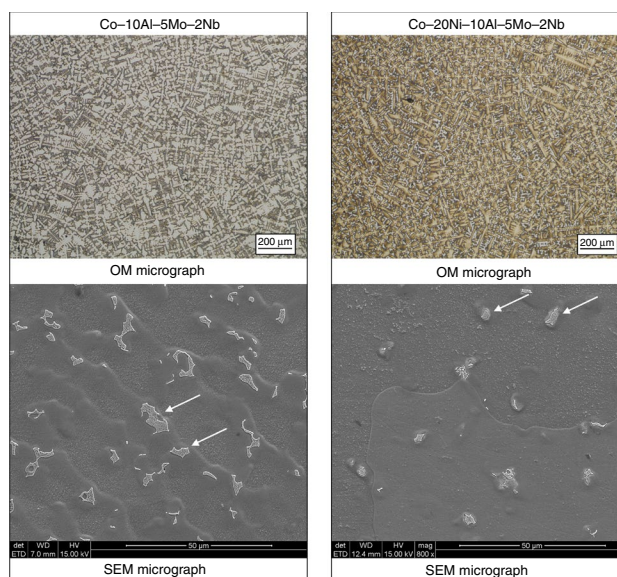


Fig. 1 OM and SEM images of primary microstructure of Co–(Ni)–Al–Mo–Nb alloys

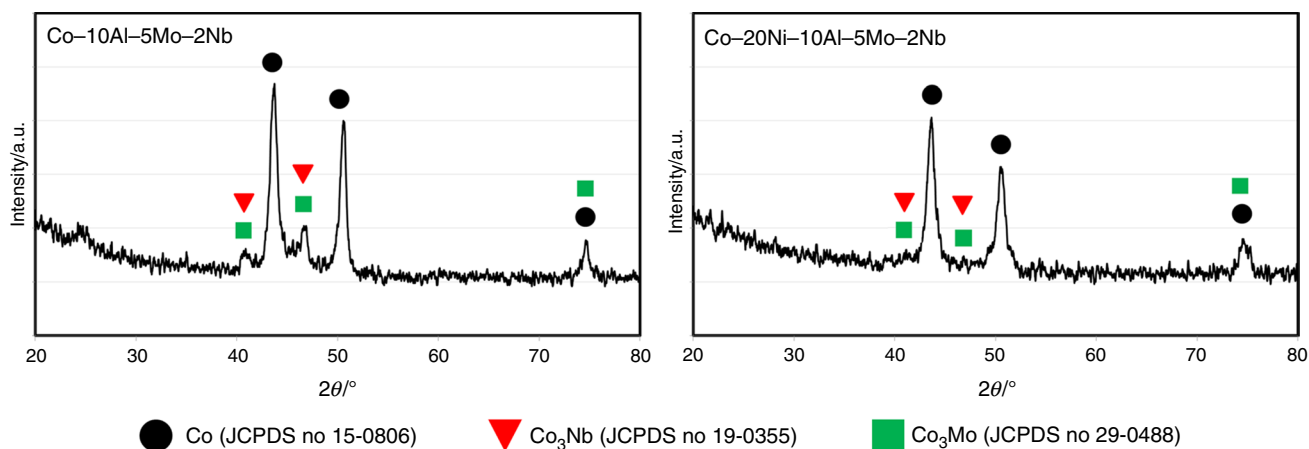


Fig. 2 X-ray diffraction patterns Co–(Ni)–Al–Mo–Nb alloys in as-cast state

discussed phases are lower compared to those of Ni-free alloy. Furthermore, the microstructural analysis showed lower concentration of the interdendritic precipitates for alloy with Ni compared to that of Co–10Al–5Mo–2Nb (at%).

After short characterization of the as-cast microstructure, the analyzed castings were subjected to the differential thermal analysis. Figure 3 shows the DTA curves corresponding to the first, Ni-Free alloy. The heating curve did not show any distinct thermal effects up to 1300 °C. One

substantial endothermic effect that corresponds to the melting point of alloy may be visible in the temperature range of 1300–1400 °C. However, the course of DTA curve in this range is not sharp; therefore, the accurate determination of melting temperature could be difficult. More information concerning the thermal behavior of alloy is shown by the cooling curve. Except the *liquidus* temperature (marked by green arrow), the green DTA plot allows to observe two exothermic effects; the first one started at 1268 °C (effect is indicated by black circle), whereas the second one at 950 °C (effect is indicated by black arrow). The first thermal effect is connected with precipitation of some phase. At comparable temperature (1231 °C) takes place the eutectic reaction in Co–Nb system [16]:



The second thermal effect observed at 950 °C is typical for precipitation of the γ' phase that was observed in other publication [12]. Afterward, the analyzed specimen was subjected to the another DTA experiment under the same conditions. The course of both heating and cooling plots was comparable to that of the plots from first analysis; however, one exception occurred. The heating plot exhibits some endothermic effect at 1244 °C. Moreover, the cooling curve shows reversible effect, which is very similar to the effect that occurred in the first analysis (at 1268 °C). These results imply that the phase which precipitated at 1268 °C in the first analysis was dissolved at 1244 °C in the second analysis and then again precipitated in the cooling process.

Figure 4 shows DTA analysis of Co–20Ni–10Al–5Mo–2Nb (at%) alloy. The course of DTA curves is similar to that of Ni-free alloy; however, no effects connected with precipitation or dissolution of phases were observed above 1200 °C. The same observation may be done after observation of the second analysis. The

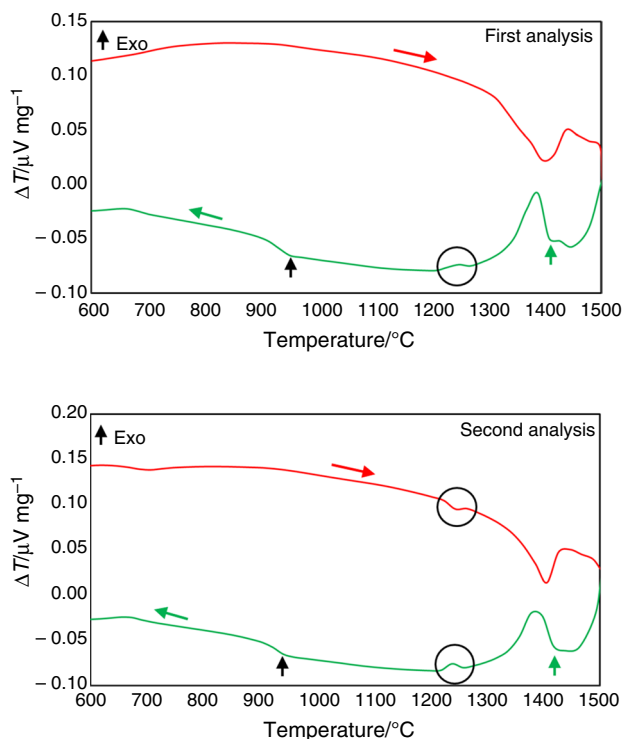


Fig. 3 Differential thermal analysis of Co–10Al–5Mo–2Nb alloy in as-cast state

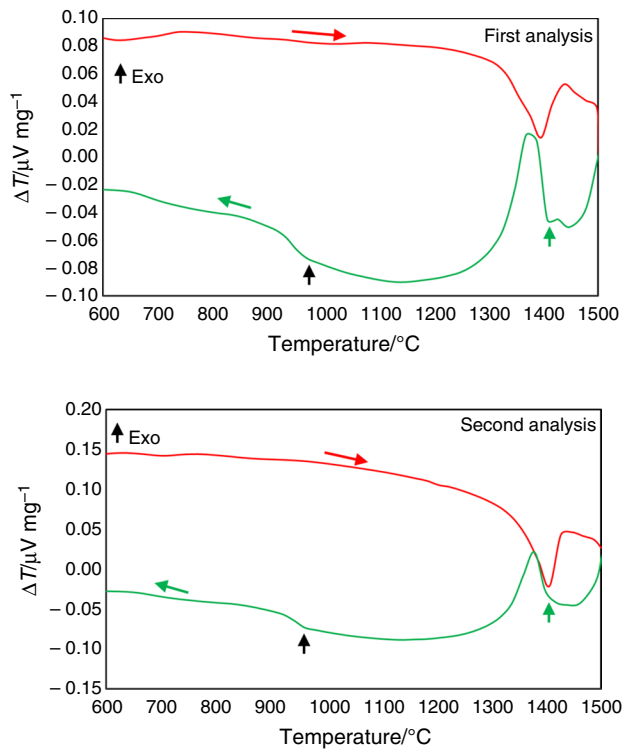


Fig. 4 Differential thermal analysis of Co-20Ni-10Al-5Mo-2Nb alloy in as-cast state

temperature of the effect corresponding to γ' precipitation is comparable for both alloys.

Afterward, the W-free Co-based superalloys were solution heat-treated at 1200 °C. The OM micrographs as well as SEM/EDS analysis of as-solutionized alloys are shown in Fig. 5. The micrographs made by optical microscopy show microstructure of the alloys after solution heat treatment. The as-solutionized alloys were characterized by grainy microstructure, whereas the size of grains was several hundred μm . After solutionizing of the alloys at 1200 °C, all phases observed in the as-cast state were dissolved which is confirmed by SEM micrographs. The measurement of chemical composition in micro-areas by EDS method shows that the chemical composition is in well accordance with the nominal one.

After the first heat treatment operation, the alloys were analyzed via DTA another time. Figure 6 shows the DTA plots corresponding to Co-10Al-5Mo-2Nb (at%) in the as-solutionized state. The heating curve exhibits the endothermic effect at 866 °C that corresponds to order–disorder transformation related to the γ' phase. In the case of alloy after solution heat treatment, the melting effect is clearer and starts at 1313 °C. Furthermore, the cooling plot shows an exothermic effect that starts at 1248 °C. This

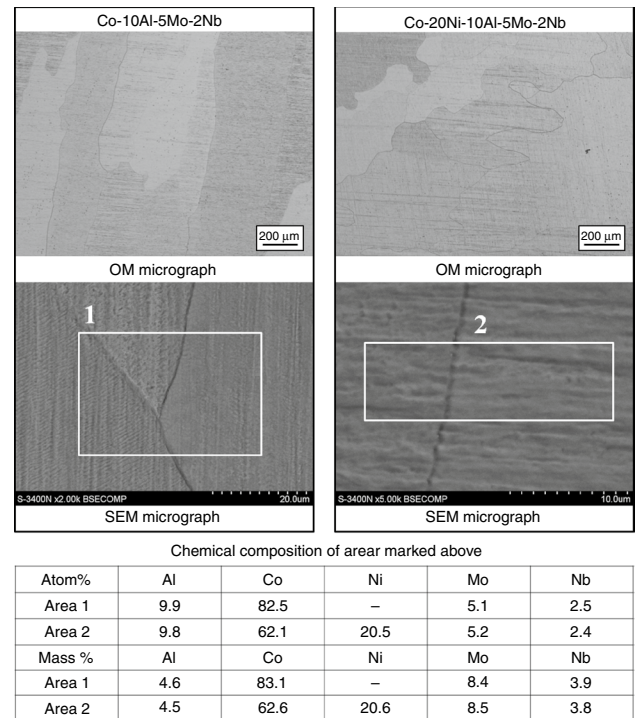


Fig. 5 Microstructure of Co-(Ni)-Al-Mo-Nb alloys in as-solutionized state

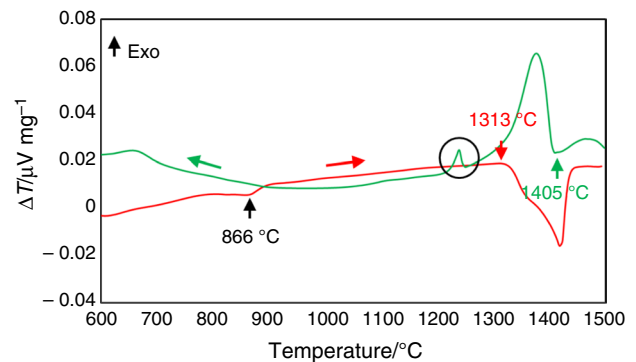


Fig. 6 Differential thermal analysis of Co-10Al-5Mo-2Nb alloy in as-solutionized state

effect was reported in the as-cast state. Moreover, the cooling plot did not reveal any effect corresponding to the γ' precipitation that was unexpected. The thermal analysis of Co-20Ni-10Al-5Mo-2Nb (at%) alloy is be seen in Fig. 7. The course of heating curve is analogous to that of heating plot of Ni-free alloy; however, the order–disorder transformation occurred at c.a. 100 °C higher temperature. The cooling plot did not reveal any precipitation effect, even the γ' precipitation that was also surprising. In order to verify the

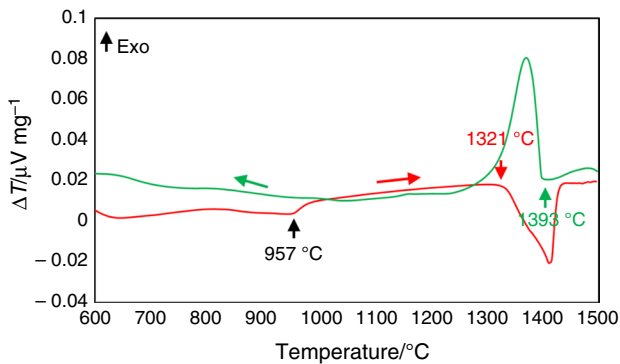


Fig. 7 Differential thermal analysis of Co–20Ni–10Al–5Mo–2Nb alloy in as-solutionized state

temperature of thermal effects connected with dissolution of the γ' phase, aging operations at different temperatures were performed for both alloys.

Figure 8 shows example SEM micrograph of Co–20Ni–10Al–5Mo–2Nb (at%) alloy after aging. The microstructure composed of tiny cuboidal γ' precipitates is typical for such alloys after the precipitation hardening. In order to rate effectiveness of the aging, the hardness measurements were carried out (Fig. 9). The hardness of Ni-free alloy in the as-cast state measured by the Vickers method was 238 HV2.5, whereas after the solution heat treatment, the hardness value decreased to 206 HV2.5. After 5 h of aging at 800 °C, the hardness of alloy reached c.a. 303 HV2.5. This result implies that the γ – γ' microstructure was obtained in this case. The aging operation in the temperature range of 850–1000 °C resulted in substantially lower hardness compared to that of after aging at 800 °C. Therefore, temperature 850 °C and the higher ones could be too high for heat treatment and operation of this alloy, which is in accordance with the DTA analysis (Fig. 6), which revealed the effect related to dissolution of the γ' at 866 °C. In the case of Co–20Ni–10Al–5Mo–2Nb (at%) alloy, the value of hardness in the as-cast state was c.a. 257 HV2.5, whereas the solutionizing of alloy at 1200 °C decreased hardness to 237 HV2.5. The increase in hardness measured by Vickers method to c.a. 317 HV2.5 was noted for the specimen aged at 800 °C. High hardness was measured also after aging at 850 °C and 900 °C and reached c.a. 313 HV2.5 in both cases. The value of hardness of specimen aged at 950 °C was 218 HV2.5, whereas after aging at 1000 °C, the value of hardness was c.a. 213 HV2.5. The obtained results imply that temperature 950 °C too created the γ – γ' microstructure in this alloy, which is in accordance with noticed endothermic thermal effect (Fig. 7) that implies the dissolution of γ' at 957 °C.

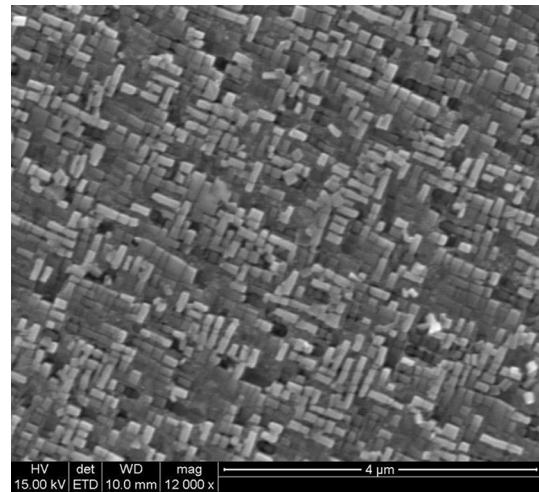


Fig. 8 SEM micrograph of Co–20Ni–10Al–5Mo–2Nb alloy after aging at 900 °C

After aging, the thermal analysis was performed in order to investigate the *solvus* and *solidus* temperatures of alloys. Figure 10 shows the DTA plots of Co–10Al–5Mo–2Nb (at%) alloy after aging at 800 °C for 5 h. The heating curve revealed three endothermic effects. The first one at 857 °C corresponds to the order–disorder transformation, which indicates the *solvus* temperature. The second effect that occurred at 1175 °C is similar to the effects observed earlier (Fig. 3); however, in this case, the endothermic effect occurred at lower temperature. The third effect is connected with start of alloy's melting, namely the *solidus* temperature, which is 1318 °C for the discussed alloy. The melting start effect corresponding to the *solidus* temperature is substantially lower compared to that of melting temperature of Co–9Al–9W (at%) alloy (1447 °C) [12]. The cooling curve showed that precipitation of the γ' starts at 845 °C that is similar compared to the temperature of dissolution. It is worth to notice that effect related to the γ' precipitation was recorded at substantially lower temperature compared to that of as-cast state. The thermal analysis of Co–20Ni–10Al–5Mo–2Nb (at%) alloy is shown in Fig. 11. In this case, the *solvus* temperature according to the heating curve is 944 °C. Furthermore, the melting point of alloy according to DTA analysis is 1338 °C. It is worth to notice that the exothermic effect connected with precipitation of the γ' occurred at 846 °C that is almost 100 °C lower compared to that of analogous effect on heating curve. Therefore, the DSC analysis was performed in order to precisely investigate the thermal effect connected with ordering of γ' phase. Figure 12 shows the DSC plots corresponding to Co–10Al–5Mo–2Nb (at%) alloy after aging at 800 °C for

Fig. 9 Vickers hardness of Co–(Ni)–Al–Mo–Nb alloys after different heat treatment operations

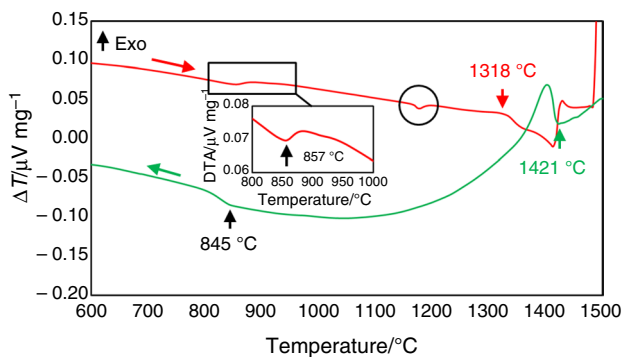
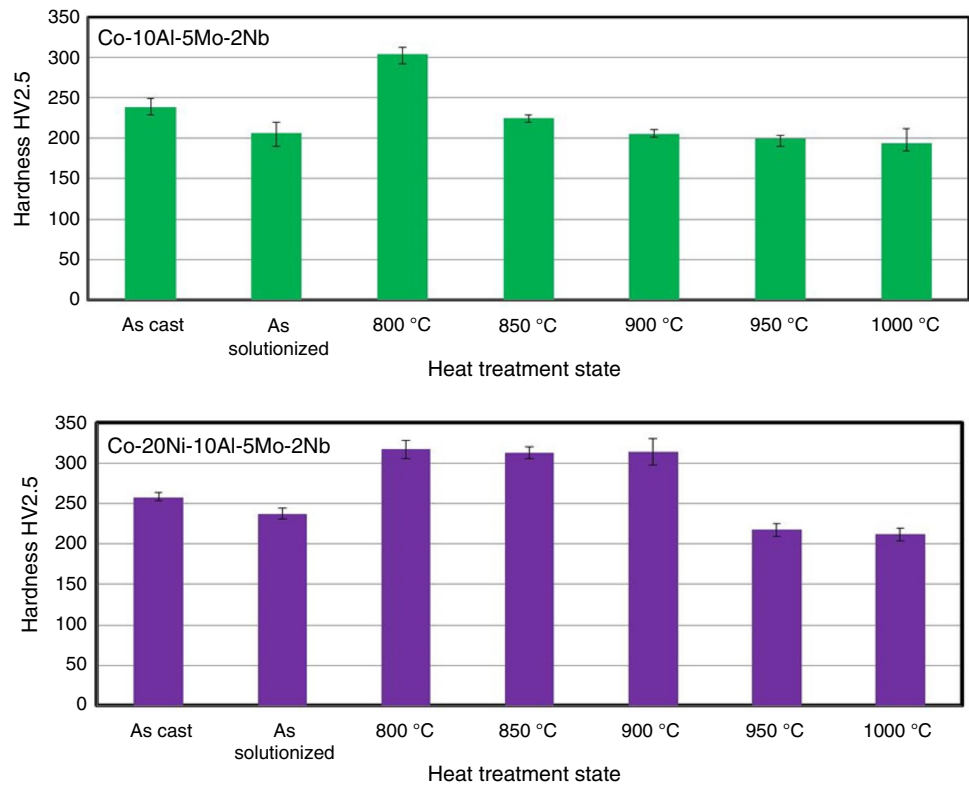


Fig. 10 Differential thermal analysis of Co–10Al–5Mo–2Nb alloy after aging at 800 °C

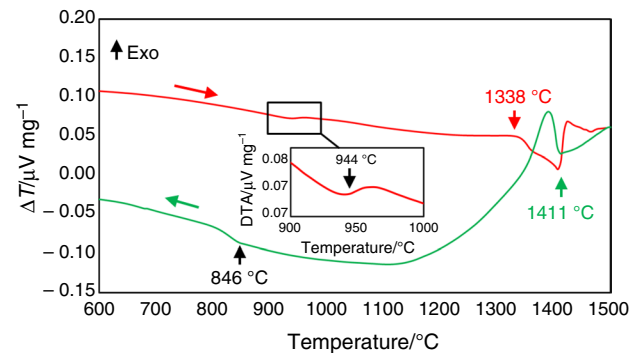


Fig. 11 Differential thermal analysis of Co–20Ni–10Al–5Mo–2Nb alloy after aging at 800 °C

5 h. The solvus temperature determined using heating curve (861 °C) was close to that of indicated by DTA (Fig. 8), whereas the temperature of reversible effect during cooling (845 °C) was almost the same in the case of DTA and DSC methods. Furthermore, some endothermic effect (indicated by black circle) was observed at 718 °C. Such peak is characteristic for magnetic transformation in cobalt and its alloys. Cooling curve showed reversible effect; however, its

intensity was slight. Figure 13 shows the analogous DSC analysis of alloy containing Ni. In this case, the *solvus* temperature indicated by the heating curve was 950 °C. The cooling curve showed the exothermic effect related to formation of the γ' phase at 942 °C. The effects connected with magnetic transformation were observed also in this case.

Fig. 12 Differential scanning calorimetry of Co-10Al-5Mo-2Nb alloy after aging at 800 °C

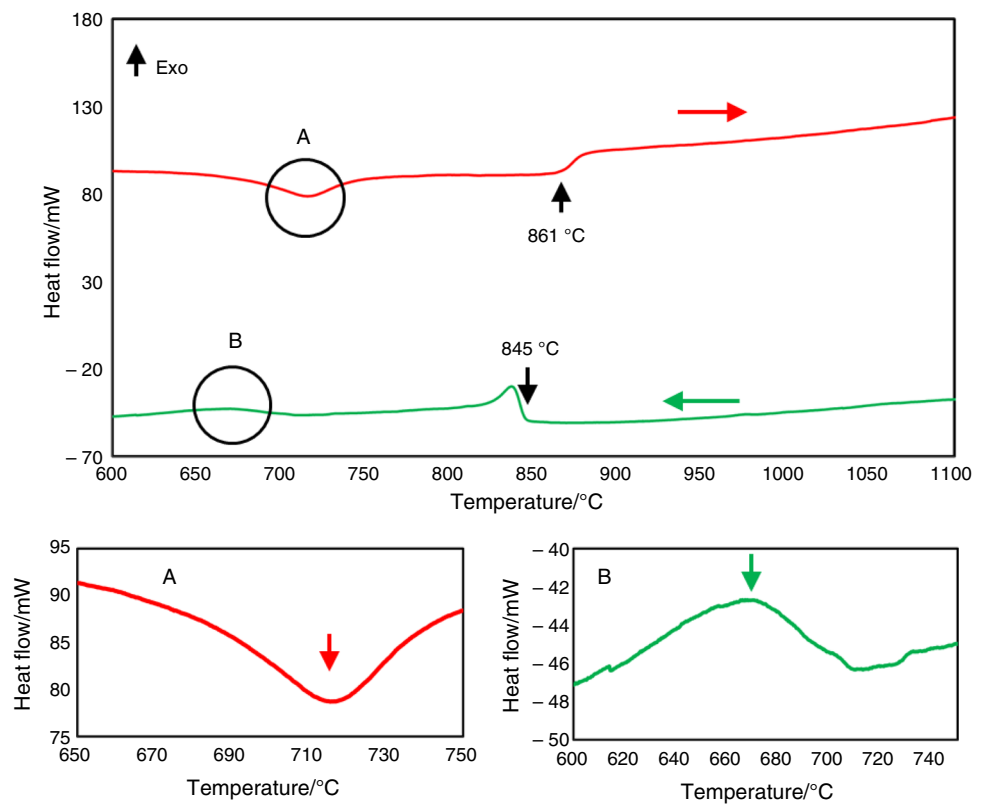
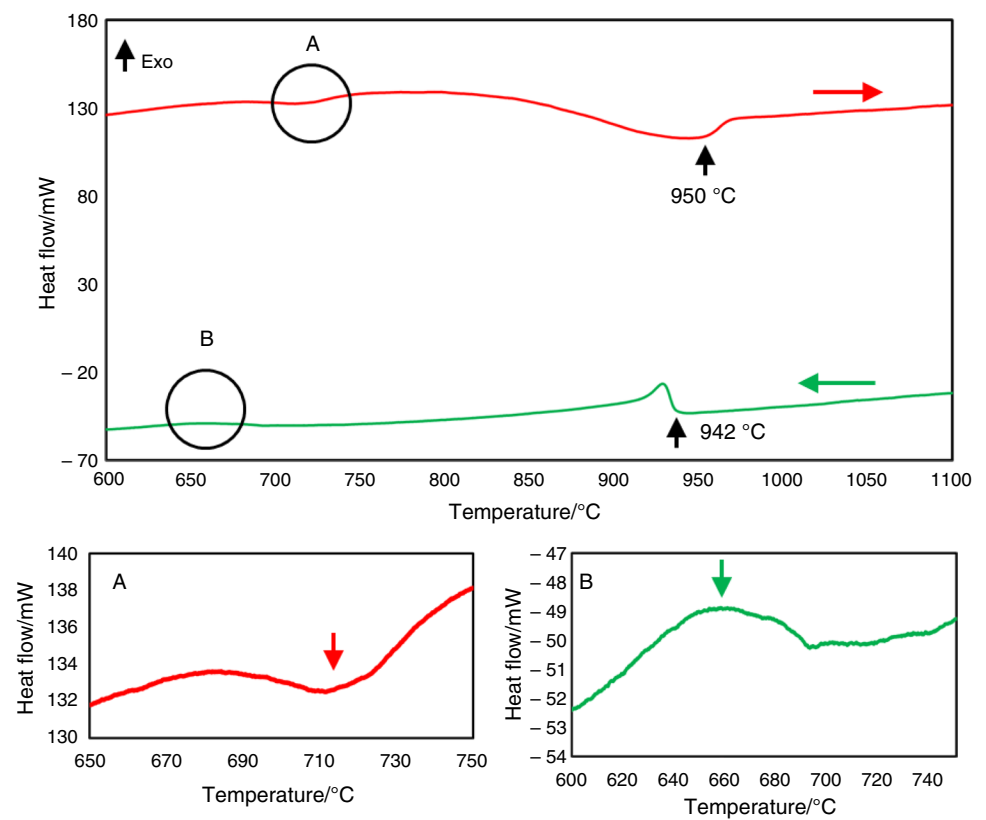


Fig. 13 Differential scanning calorimetry of Co-20Ni-10Al-5Mo-2Nb alloy after aging at 800 °C



Conclusions

The presented analysis revealed many different thermal effects related to different structural processes in W-free cobalt superalloys based on Co–Al–Mo–Nb and Co–Ni–Al–Mo–Nb systems. The first difference between Co–(Ni)–Al–W alloys and alloys containing Mo and Nb was in the primary microstructure. In the case of W-free alloys, some detrimental Mo- and Nb-rich phases were observed in the interdendritic areas. Moreover, the thermal analysis revealed precipitation of some phases in the temperature range of 1200–1250 °C. Except microstructural aspect, W-replacement affected the thermal behavior of alloys.

The *solidus* temperature of both W-free alloys was about 100 °C lower compared to that of Co–9Al–9W (at%) alloy [12]. Substitution of W by Mo and Nb allows to obtain the γ – γ' microstructure. However, the *solvus* temperature (861 °C) for Co–Al–Mo–Nb alloy is substantially lower compared to that of Co–Al–W alloys (~990 °C) [2]. Moreover, the γ' phase is not stable during long-term annealing [14] and requires stabilization by other elements.

The *solvus* temperature For Co–20Ni–10Al–5Mo–2Nb (at%) alloy was c.a. 90 °C higher compared to that of Ni-free Co-based alloy. It is in accordance with fact that nickel alloying extends the range of γ' occurrence in Co-alloys [17]. Furthermore, the *solidus* temperature of Ni-containing alloy was slightly higher compared to that of Co–10Al–5Mo–2Nb (at%).

Acknowledgements This work was supported by National Science Centre (Project 2018/29/N/ST8/02062). Publication was supported by the Rector's Grant in the field of research and development, Silesian University of Technology, Grant Number 11/030/RGJ19/0234.

Open Access This article is licensed under a Creative Commons Attribution 4.0 International License, which permits use, sharing, adaptation, distribution and reproduction in any medium or format, as long as you give appropriate credit to the original author(s) and the source, provide a link to the Creative Commons licence, and indicate if changes were made. The images or other third party material in this article are included in the article's Creative Commons licence, unless indicated otherwise in a credit line to the material. If material is not included in the article's Creative Commons licence and your intended use is not permitted by statutory regulation or exceeds the permitted use, you will need to obtain permission directly from the copyright holder. To view a copy of this licence, visit <http://creativecommons.org/licenses/by/4.0/>.

References

- Lee CS. Precipitation-hardening characteristics of ternary cobalt–aluminum–X alloys. Tucson: University of Arizona; 1971.
- Sato J, Omori T, Oikawa K, Ohnuma I, Kainuma R, Ishida K. Cobalt-base high-temperature alloys. *Science*. 2006;312:90–1.
- Makineni SK, Nithin B, Chattopadhyay K. A new tungsten-free γ – γ' Co–Al–Mo–Nb-based superalloy. *Scr Mater*. 2014;98:36–9.
- Nithin B, Samanta A, Makineni SK, Alam T, Pandey P, Abhishek K, Banerjee R, Chattopadhyay K. Effect of Cr addition on γ – γ' cobalt-based Co–Mo–Al–Ta class of superalloys: a combined experimental and computational study. *J Mater Sci*. 2017;52:11036–47.
- Epishin A, Petrushin N, Nolze G, Gerstein G, Maier HJ. Investigation of the γ' -strengthened quaternary co-based alloys Co–Al–W–Ta. *Metall Mater Trans*. 2018;49A:4042–57.
- Bocchini PJ, Sudbrack ChK, Noebe RD, Seidman DN. Temporal evolution of a model Co–Al–W superalloy aged at 650°C and 750°C. *Acta Mater*. 2018;159:197–208.
- Pyczak F, Bauer A, Göken M, Lorenz U, Neumeier S, Oehring M, Paul J, Schell N, Schreyer A, Stark A, Symanzik F. The effect of tungsten content on the properties of L12-hardened Co–Al–W alloys. *J Alloys Compd*. 2015;632:110–5.
- Zenk CH, Neumeier S, Stone HJ, Göken M. Mechanical properties and lattice misfit of γ – γ' strengthened Co-base superalloys in the Co–W–Al–Ti quaternary system. *Intermetallics*. 2014;55:28–39.
- Bocchini PJ, Sudbrack ChK, Sauza DJ, Noebe RD, Seidman DN, Dunand DC. Effect of tungsten concentration on microstructures of Co–10Ni–6Al–(0,2,4,6)W–6Ti (at%) cobalt-based superalloys. *Mater Sci Eng, A*. 2017;700:481–6.
- Xue F, Wang M, Feng Q. Alloying effects on heat-treated microstructure in Co–Al–W-base superalloys at 1300°C and 900°C. In: Huron ES, Reed RC, Hardy MC, Mills MJ, Montero RE, Portella PD, Telesman J, editors. *Superalloys 2012, 12th international symposium on superalloys*. Pittsburgh: TSM (The Minerals, Materials & Metals Society); 2012. p. 813–21.
- Bocchini PJ, Sudbrack ChK, Noebe RD, Dunand DC, Seidman DN. Effects of titanium substitutions for aluminum and tungsten in Co–10Ni–9Al–9 W (at%) superalloys. *Mater Sci Eng, A*. 2017;705:122–32.
- Tomaszewska A, Moskal G, Migas D, Mikuškievicz M, Maciąg T. Thermal parameters determination of Co–Al–W as-cast alloy homogenization by DTA analysis. *J Therm Anal Calorim*. 2018;134:157–64.
- Makineni SK, Nithin B, Chattopadhyay K. Synthesis of a new tungsten-free γ/γ' cobalt-based superalloy by tuning alloying additions. *Acta Mater*. 2015;85:85–94.
- Makineni SK, Nithin B, Chattopadhyay K. Phase evolution and crystallography of precipitates during decomposition of new “tungsten-free” Co(Ni)–Mo–Al–Nb γ – γ' superalloys at elevated temperatures. *J Mater Sci*. 2016;51:7843–60.
- Mikuszewski T, Tomaszewska A, Moskal G, Migas D, Niemiec D. Primary microstructure characterization of new type γ – γ' Co–Al–W cobalt-based superalloys. *Mater Eng*. 2017;5:217–23.
- Hari Kumar KC, Ansara I, Wollants P, Delaey L. Thermodynamic optimisation of the Co–Nb system. *J Alloys Compd*. 1998;267:105–12.
- Li W, Li L, Stoichko A, Feng Q. Effective design of a Co–Ni–Al–W–Ta–Ti alloy with high γ' solvus temperature and microstructural stability using combined CALPHAD and experimental approaches. *Mater Des*. 2019;180:107912.

Publisher's Note Springer Nature remains neutral with regard to jurisdictional claims in published maps and institutional affiliations.